JACS
JOURNAL OF THE AMERICAN CHEMICAL SOCIETY
Communication
pubs.acs.org/JACS

Deep Absorbing Porphyrin Small Molecule for High-Performance Organic Solar Cells with Very Low Energy Losses

Ke Gao,[†] Lisheng Li,[†] Tianqi Lai,[†] Liangang Xiao,[†] Yuan Huang,[†] Fei Huang,[†] Junbiao Peng,[†] Yong Cao,[†] Feng Liu,*[,‡] Thomas P. Russell,[‡,¶] René A. J. Janssen,*[,§] and Xiaobin Peng*[,†]

[†]State Key Laboratory of Luminescent Materials and Devices, South China University of Technology, 381 Wushan Road, Guangzhou, 510640, P. R. China

[‡]Materials Sciences Division, Lawrence Berkeley National Laboratory, Berkeley, California 94720, United States

[¶]Polymer Science and Engineering Department, University of Massachusetts, Amherst, Massachusetts 01003, United States

[§]Molecular Materials and Nanosystems, Eindhoven University of Technology, PO Box 513, 5600 MB Eindhoven, The Netherlands

Supporting Information

ABSTRACT: We designed and synthesized the DPPEZnP-TEH molecule, with a porphyrin ring linked to two diketopyrrolopyrrole units by ethynylene bridges. The resulting material exhibits a very low energy band gap of 1.37 eV and a broad light absorption to 907 nm. An open-circuit voltage of 0.78 V was obtained in bulk heterojunction (BHJ) organic solar cells, showing a low energy loss of only 0.59 eV, which is the first report that small molecule solar cells show energy losses <0.6 eV. The optimized solar cells show remarkable external quantum efficiency, short circuit current, and power conversion efficiency up to 65%, 16.76 mA/cm^2, and 8.08%, respectively, which are the best values for BHJ solar cells with very low energy losses. Additionally, the morphology of DPPEZnP-TEH neat and blend films with $PC_{61}BM$ was studied thoroughly by grazing incidence X-ray diffraction, resonant soft X-ray scattering, and transmission electron microscopy under different fabrication conditions.

Solution-processed organic solar cells (OSCs) are promising renewable energy sources that have attracted much interest recently.[1] The power conversion efficiencies (PCEs) of OSCs have surpassed the 10% barrier for single junction devices and are expected to be higher for tandem devices.[2] In comparison to polymeric materials, small molecules (SMs) have the advantages of well-defined structures and molecular weights. SMs are easy to purify and have good batch-to-batch reproducibility, enriching the material choices for commercialization of OSCs.[3]

To enhance the performance of OSCs, chemists in photovoltaics have been trying to extend the material's absorption to long wavelength, >800 nm (i.e., very low energy band gap E_g), to absorb more light. However, it is difficult to design highly efficient organic materials including polymer and SM donors that show very low energy band gaps and high open-circuit voltages (V_{oc}) for OSCs simultaneously. The energy loss (E_{loss}), which connects E_g and V_{oc}, defined as $E_{loss} = E_g - eV_{oc}$, is an important parameter to evaluate solar cells.[4] Low E_{loss} values, <0.5 eV in highly efficient perovskite solar cells (PSCs) and 0.34−0.48 eV for the best inorganic crystalline solar cells,[5] enhance the energy efficiency by which photons are converted into collectable charges[4] and thus can lead to high-performance photovoltaic devices. For bulk heterojunction (BHJ) OSCs, the minimum E_{loss} was suggested to be 0.6 eV,[4] and the corresponding V_{oc} is often used as the maximum achievable V_{oc}. However, E_{loss} < 0.6 eV is still rare even for PSCs[6] and has not been reported for SM-based OSCs. It also should be noted that, though PSCs sometimes gave energy losses <0.6 eV, their performance often dropped dramatically at such low E_{loss} values.[6]

For a SM, the limited backbone length restricts linear extension of conjugation, which retards absorption in the longer wavelength region. Strong donor−acceptor (D-A) pairs can extend absorption, but the energy level offsets sacrifice V_{oc}.[7] To date, the most efficient SMs were built on oligothiophenes, with limited absorption but high V_{oc},[2b,8] or D-A hybrids, with broader absorption and high current but limited V_{oc}.[9] Extracting more energy from BHJ blends requires simultaneously enhancing photocurrent and voltage, which relies on further optimizing both the electron-donating materials and the BHJ morphology. New design of both polymers and SMs that can extend photon absorption to >800 nm, while maintaining high V_{oc} and high PCE, will be the next major advance in OSCs with either single junction or tandem structures.

Porphyrin analogues have extensive π-conjugated surfaces and show high efficiency in photosynthesis.[10] In this work, two diketopyrrolopyrrole (DPP) units are linked to both sides of a porphyrin core to extend the π-conjugation via an ethynylene bridge, serving two functions:[11] introducing sp^1 carbon hybridization can lower the highest occupied molecular orbital (HOMO) energy level of the target materials, since there are more s-orbital components, and its fluent cylinder-like π-electron density is more adaptable to conformational and steric constraints, thus enhancing intermolecular π-π stacking and facilitating intramolecular charge transport. Since it has been reported that thienyl substituents can enhance OSCs' performance, two thienyl groups with a 2-ethylhexyl substituent are introduced into the porphyrin core, with an added benefit of improving the material's solubility.

The target molecule 5,15-bis(2,5-bis(2-ethylhexyl)-3,6-dithienyl-2-yl-2,5-dihydro-pyrrolo[3,4-*c*]pyrrole-1,4-dione-5′-yl-

Received: April 17, 2015
Published: June 2, 2015

DOI: 10.1021/jacs.5b03740
J. Am. Chem. Soc. 2015, 137, 7282−7285

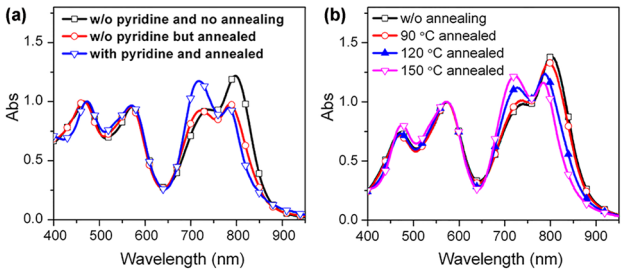

Figure 1. UV-vis-NIR absorption spectra of DPPEZnP-TEH (a) thin and (b) BHJ films.

ethynyl)-10,20-bis(5-(2-ethylhexyl)thienyl)porphyrin zinc(II) (DPPEZnP-TEH) was synthesized by a Sonogashira coupling reaction (Supporting Information (SI)), affording 75% of the final product, with added benefits of avoiding toxic stannyl intermediates and potential chemical accidents from lithiation reactions in the synthetic routes. The absorption spectra of DPPEZnP-TEH in solution and in thin film showed a broad spectral coverage in the visible and near-infrared (NIR) regions (Figure S3). In very dilute dichloromethane solution, three strong absorption peaks at 466, 568, and 727 nm were observed. Such strong absorption in the NIR region at a short backbone length indicates that the π-electron delocalization between constituent units is very effective. This is due partially to the ethynylene bridge and partially to the large aromatic surface that extends the conjugation. In thin film, DPPEZnP-TEH exhibited red-shifted absorption peaks at 472, 573, and 802 nm with a shoulder peak at 739 nm. The significant red-shift of 75 nm from 727 nm in solution to 802 nm in film is attributed to the strong intermolecular π-π stacking in the solid state, possibly due to the optically active J-aggregation.[12] The optical band gap of the solid thin film is calculated to be 1.37 eV based on the onset of the absorption spectra (907 nm).

Thermal annealing was applied to DPPEZnP-TEH thin film (Figure 1a). The intensity of the 802 nm peak decreased under thermal treatment, and the peak center shifted slightly to shorter wavelength (786 nm). Annealing also induced a new peak at 720 nm, which intensified at elevated temperature. This new optical state possibly came from H-aggregation of DPPEZnP-TEH molecules, more than likely formed by sliding the intermolecular π-π stacking, changing from J- to H-aggregation. The absorption spectrum of DPPEZnP-TEH/[6,6]-phenyl-C_{61}-butyric acid methyl ester ($PC_{61}BM$) blend (1:1.2, w/w) thin films was also investigated. Chlorobenzene (CB)-cast thin films showed a dominant peak at 798 nm with a shoulder at 732 nm (Figure 1b). Under thermal annealing, the 798 nm peak decreased and blue-shifted to 786 nm, and the shoulder at 732 nm increased and blue-shifted to 722 nm, which was the same trend as with pure DPPEZnP-TEH film. More significant reduction of the 798 nm peak to 783 nm and increase of the 722 nm peak to 718 nm were observed for the blend films with $PC_{61}BM$ prepared in the presence of a pyridine additive and then under thermal annealing.

Cyclic voltammetry measurements were carried out to estimate the HOMO and the lowest unoccupied molecular orbital (LUMO) energy levels of DPPEZnP-TEH. As shown in Figure S4, the onset oxidation (E_{ox}) and reduction (E_{red}) potentials of DPPEZnP-TEH were 0.82 and −0.56 V vs Ag/AgCl electrode, respectively. The formal potential of the Fc/Fc^+ vs Ag/AgCl electrode was recorded to be 0.48 V in this work, from which the HOMO and the LUMO energy levels were estimated to be −5.14 and −3.76 eV according to the empirical formulas

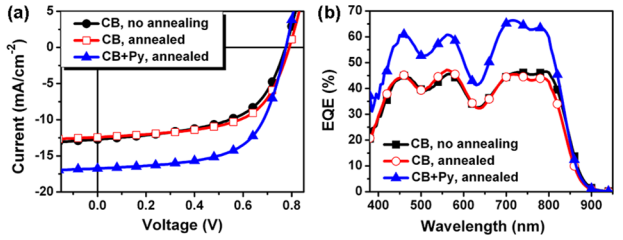

Figure 2. (a) J−V curves and (b) EQE of the OSCs using DPPEZnP-TEH:$PC_{61}BM$ (1:1.2, w/w) active layer.

Table 1. Summary of Device Performances

devices	J_{sc} (mA/cm^2)	V_{oc} (V)	FF (%)	PCE[a] (%)
as cast	12.72	0.78	55.76	5.53 (5.47)
annealed	12.44	0.79	59.90	5.89 (5.82)
Py-annealed	16.76	0.78	61.80	8.08 (8.04)

[a]Values in parentheses are the average PCE obtained from 20 devices.

$E_{HOMO} = -e(E_{ox} + 4.32)$ (eV) and $E_{LUMO} = -e(E_{red} + 4.32)$ (eV).[13] The electrochemical energy band gap was 1.38 eV, almost the same as the optical energy gap calculated from the onset of the absorption spectrum in film.

Solution-processed BHJ OSCs were fabricated utilizing $PC_{61}BM$ as the electron acceptor and DPPEZnP-TEH as the electron donor under a conventional device structure of ITO/PEDOT:PSS/active layer/PFN/Al [ITO = indium tin oxide; PEDOT:PSS = poly(3,4-ethylenedioxythiophene):poly(styrenesulfonate); PFN = poly[(9,9-bis(30-(*N*,*N*-dimethylamino)-propyl)-2,7-fluorene)]-*alt*-2,7-(9,9-dioctylfluorene)] and then measured under AM 1.5 illumination. The optimized ratio of DPPEZnP-TEH and $PC_{61}BM$ was 1:1.2 (w/w). Device results are summarized in Figure 2 and Table 1. An exceptionally high V_{oc} = 0.78 V was obtained for the devices processed under different conditions, indicating a suitable alignment of the $HOMO_{DPPEZnP\text{-}TEH}$ and $LUMO_{PCBM}$. It is worth commenting that the photon energy loss of E_{loss} = 0.59 eV is the first report for SM-based BHJ OSCs, and E_{loss} values <0.6 eV are still rare even for PSCs. Since the minimum E_{loss} has previously been suggested to be 0.6 eV and the corresponding V_{oc} is also often used as the maximum achievable in BHJ OSCs, the 0.59 eV energy loss of DPPEZnP-TEH:$PC_{61}BM$ OSCs is very low, and thus V_{oc} = 0.78 V is very high for materials with a low energy band gap of only 1.37 eV.

The BHJ devices fabricated without solvent additive and without thermal annealing exhibited a good PCE of 5.53% with a short circuit current (J_{sc}) of 12.72 and a fill factor (FF) of 55.76%. When the OSCs were thermally annealed at 120 °C for 10 min, only slight performance enhancements of FF to 59.9% and PCE to 5.89% were observed. The devices fabricated in the presence of 1% pyridine additive and then thermally annealed showed drastic enhancements in PCE to 8.08%, J_{sc} to 16.76 mA/cm^2, and FF to 61.8%, at an almost unchanged V_{oc} = 0.78 V. J_{sc} = 16.76 mA/cm^2 is the highest for SM-based solar cells, and PCE = 8.08% makes DPPEZnP-TEH one of the top-tier light-harvesting molecules.

Compared to the alkoxy phenyl groups we reported previously, the effects of the alkylthienyl groups are two-fold: deepening the E_{HOMO} (demonstrated by density functional theory optimizations (SI), electrochemical and absorption measurements, and the slightly higher V_{oc}) and changing from J- to H-aggregation when the films are prepared in the presence of pyridine additive and then thermally annealed. It was reported that the amount of

DOI: 10.1021/jacs.5b03740
J. Am. Chem. Soc. 2015, 137, 7282−7285

H-aggregate should be considerably larger than the J-aggregate to improve cell performance.[14]

The external quantum efficiencies (EQEs) of the devices were measured, showing a broad-spectrum response from 380 to 907 nm. CB-processed devices showed EQE ≈ 45% over a broad range. No large differences were seen with thermally annealed devices. However, pyridine additive significantly elevated the EQE to 65%. Single carrier devices were also fabricated. The hole mobilities of the blend and pure DPPEZnP-TEH films were calculated to be 4.85×10^{-4} and 1.12×10^{-3} cm^2 V^{-1} s^{-1}, respectively, by the space charge limited current method,[15] similar to those of other of high-performance systems.[8c]

It should be noted that, though low energy loss for OSCs <0.6 eV was reported for PSCs, the quantum yield for charge generation often drops dramatically for E_{loss} < 0.5 eV.[4,11b] In the current case, the photovoltaic parameters of EQE, J_{sc}, and PCE remained at very high levels simultaneously, all being the highest values within the 0.6 eV E_{loss} barrier, indicating the possibility of synergic material design to simultaneously enhance performances.

Several conditions are known to reduce E_{loss} and give high V_{oc}.[16] The permittivity of DPPEZnP-TEH is 3.9 at 10 kHz, which is larger than the values of three well-known OPV materials (SI) and similar to that of a previously synthesized material,[9g] suggesting that the large permittivity can contribute to the very low E_{loss} of porphyrin-based OSCs.[16a] However, the free base porphyrin ($DPPEH_2P$-TEH, SI) shows a permittivity of only 3.1, and its optical band gap is 1.32 eV. The OSCs based on $DPPEH_2P$-TEH as the donor and $PC_{61}BM$ as the acceptor exhibit a PCE of only 2.52% with V_{oc} = 0.74 V (SI), and their E_{loss} = 0.58 eV is the same as that of DPPEZnP-TEH. These results indicate that that the low E_{loss} for these OSCs is closely related to the molecular constitution of the conjugated plane, and the central Zn(II) in DPPEZnP-TEH helps to improve the FF and J_{sc} of OSC devices, which could be also a consequence of morphology improvement.

Different processing conditions can lead to variations in J_{sc} and FF, and an improved morphology usually gives rise to enhanced device performance, pointing out the importance of morphology optimization in OSCs. The morphological properties of DPPEZnP-TEH in pure and blend films with $PC_{61}BM$ were characterized by grazing incidence X-ray diffraction (GIXD, Figure 3). In pure film, a weak diffraction ring at ~0.32 $Å^{-1}$ (1.96 nm) and a broad ring at ~1.48 $Å^{-1}$ (0.42 nm) were observed. The low q diffraction peak arose from the alkyl-alkyl distance or (100) reflection, while the reflection at high q diffraction arose from average π-π distance. The crystallites did not show strong orientation inside the film, as evidenced by the azimuthal spreading of the (010) diffraction peak, and specular reflection of the distorted (100) peak diffraction thus cannot be used to access crystal orientation. Thermal annealing led to a slight decrease of the (100) peak area and a shifting of peak position to 0.30 $Å^{-1}$. In blends processed from CB, a better-defined (100) diffraction peak was observed at 0.27 $Å^{-1}$ (2.32 nm) with a "crystal size" of 8.6 nm (corresponding to 3−4 stacks). A weak diffraction peak arising from PCBM was seen at 0.68 $Å^{-1}$, corresponding to a distance of 0.92 nm. The broad reflection at ~1.49 $Å^{-1}$ corresponds to the π-π stacking peak of DPPEZnP-TEH (overlapping with PCBM diffraction). The CB+Py-processed thin-film blends showed a more obvious (100) diffraction at 0.29 $Å^{-1}$ (2.17 nm). The coherence length was estimated to be 6.6 nm, corresponding to 3 stacks. The (100) peak area was slightly larger for CB+Py-processed blends, indicating a better crystallinity. The

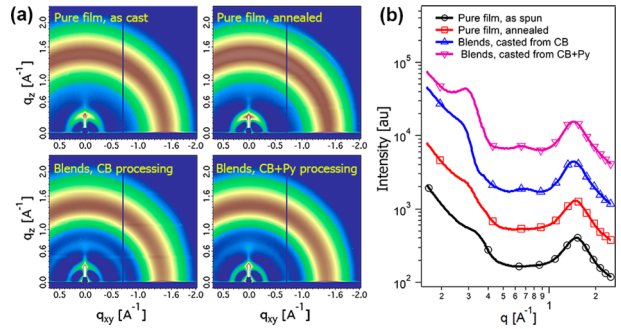

Figure 3. (a) GIXD diffractogram and (b) out-of-plane line-cut profiles of DPPEZnP-TEH pure and blend thin films.

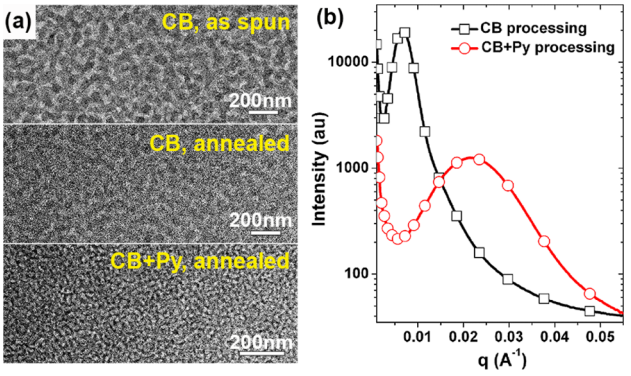

Figure 4. (a) TEM and (b) RSoXS of DPPEZnP-TEH:PCBM blends processed from different conditions.

combined GIXD and absorption investigation indicated that pyridine additive leads to enhanced crystallinity in the (100) direction with reduced crystal size. In the π-π stacking direction, the slipped J-type molecular packing was transformed to a less slipped H-type aggregation,[12c] in which the porphyrin−porphyrin interaction was enhanced. The flexibility in this transformation can be a consequence of the large aromatic surface, offering more contact area and more relative positions of stacked porphyrins that could serve as channels for carrier transport to maintain high device performance.

The morphology of the BHJ thin film was characterized by transmission electron microscopy (TEM, Figure 4a). CB-processed thin films showed an obvious phase separation with an average center-to-center distance of ~100 nm. The black and white domains are PCBM-rich and DPPEZnP-TEH-rich regions, respectively. No strong PCBM aggregation was seen in this sample, and the device had J_{sc} = 12.72 mA/cm^2. Thermal annealing of this sample led to a blurring of the phase image; however, the size scale of phase separation remained similar. Pyridine additive was quite effective in enhancing the order along the (100) direction in this system. A 1% pyridine solution strongly changed the morphology of the resulting thin film. A much finer phase separation was observed, with a characteristic size scale of ~30 nm. This sharp reduction in length scale led to a 35% increase in photocurrent, reaching 16.76 mA/cm^2.

Resonant soft X-ray scattering (RSoXS, Figure 4b) was used to further confirm the morphology of these thin films, taking a carbon K-edge scattering for each sample. CB-processed thin film (annealed) showed a strong diffraction peak at 0.0066 $Å^{-1}$, corresponding to a distance of 95.2 nm; CB+Py-processed thin film (annealed) showed a broad peak at 0.0221 $Å^{-1}$, corresponding to a distance of 28.4 nm. The RSoXS results

DOI: 10.1021/jacs.5b03740
J. Am. Chem. Soc. 2015, 137, 7282−7285

were in good agreement with the TEM observations. It is worth noting that the specific inner surface area (D-A interface) is inversely proportional to the length scale of phase separation, and thus CB+Py-processed thin film will have a roughly 2× larger inner surface area. However, only a 35% J_{sc} increase was seen. The slow decay of the RSoXS profile for films prepared from CB hindered the observation of phase-separated domains of smaller length scales (see peak fitting in SI), which enhanced light extraction in blended thin films and photocurrent in CB-processed devices. The surface morphology of BHJ thin films was probed by atomic force microscopy, and it was seen that pyridine-additive-processed thin film had a smoother surface, with a RMS roughness of only 0.52 nm (Figure S15).

In summary, a new conjugated DPP-porphyrin small molecule was developed with 2-ethylhexyl-thienyl side groups at the porphyrin core. The BHJ OSCs gave high EQE, J_{sc}, FF, and PCE up to 65%, 16.76 mA/cm^2, 61.8%, and 8.08%, respectively, with a very low energy loss of only 0.59 eV. The combination of high permittivity, main chain conjugation, and good morphology delivers a good EQE and low energy loss. The central Zn(II) also plays an important role for the high PCEs of the low energy loss OSCs. Successful demonstration of this porphyrin for OSCs suggests a new methodology in material design to achieve high-performance OSCs with very low energy loss, and its superior performance will also spur further research in more complicated device settings.

■ ASSOCIATED CONTENT

Supporting Information

Experimental details and characterization data. The Supporting Information is available free of charge on the ACS Publications website at DOI: 10.1021/jacs.5b03740.

■ AUTHOR INFORMATION

Corresponding Authors

*chxbpeng@scut.edu.cn
*iamfengliu@gmail.com
*r.a.j.janssen@tue.nl

Notes

The authors declare no competing financial interest.

■ ACKNOWLEDGMENTS

This work was financially supported by grants from International Science & Technology Cooperation Program of China (2013DFG52740, 2010DFA52150), Ministry of Science and Technology (2014CB643500), and National Natural Science Foundation of China (51473053, 51073060). F.L. and T.P.R. were supported by Polymer-Based Materials for Harvesting Solar Energy (PHaSE), an Energy Frontier Research Center funded by the U.S. Department of Energy (DOE), Office of Basic Energy Sciences (DE-SC0001087). Portions of this research were carried out at beamlines 7.3.3 and 11.0.1.2 at the Advanced Light Source, and Molecular Foundary, Lawrence Berkeley National Laboratory, which was supported by the DOE, Office of Science and Office of Basic Energy Sciences.

■ REFERENCES

(1) (a) Heeger, A. J. *Adv. Mater.* **2013**, *26*, 10. (b) Krebs, F. C.; Espinosa, N.; Hösel, M.; Søndergaard, R. R.; Jørgensen, M. *Adv. Mater.* **2013**, *26*, 29.

(2) (a) Chen, C.-C.; Chang, W.-H.; Yoshimura, K.; Ohya, K.; You, J.; Gao, J.; Hong, Z.; Yang, Y. *Adv. Mater.* **2014**, *26*, 5670. (b) Kan, B.; Zhang, Q.; Li, M.; Wan, X.; Ni, W.; Long, G.; Wang, Y.; Yang, X.; Feng, H.; Chen, Y. *J. Am. Chem. Soc.* **2014**, *136*, 15529. (c) Liu, Y.; Zhao, J.; Li, Z.; Mu, C.; Ma, W.; Hu, H.; Jiang, K.; Lin, H.; Ade, H.; Yan, H. *Nat. Commun.* **2014**, *5*, 1. (d) You, J.; Dou, L.; Yoshimura, K.; Kato, T.; Ohya, K.; Moriarty, T.; Emery, K.; Chen, C.-C.; Gao, J.; Li, G.; Yang, Y. *Nat. Commun.* **2013**, *4*, 1446. (e) Liao, S.-H.; Jhuo, H.-J.; Yeh, P.-N.; Cheng, Y.-S.; Li, Y.-L.; Lee, Y.-H.; Sharma, S.; Chen, S.-A. *Sci. Rep.* **2014**, *4*, 6813.

(3) (a) Mishra, A.; Bäuerle, P. *Angew. Chem., Int. Ed.* **2012**, *51*, 2020. (b) Walker, B.; Kim, C.; Nguyen, T.-Q. *Chem. Mater.* **2011**, *23*, 470. (c) Lin, Y.; Li, Y.; Zhan, X. *Chem. Soc. Rev.* **2012**, *41*, 4245.

(4) Veldman, D.; Meskers, S. C. J.; Janssen, R. A. J. *Adv. Funct. Mater.* **2009**, *19*, 1939.

(5) Nayak, P. K.; Bisquert, J.; Cahen, D. *Adv. Mater.* **2011**, *23*, 2870.

(6) (a) Li, W.; Hendriks, K. H.; Furlan, A.; Wienk, M. M.; Janssen, R. A. J. *J. Am. Chem. Soc.* **2015**, *137*, 2231. (b) Wang, M.; Wang, H.; Yokoyama, T.; Liu, X.; Huang, Y.; Zhang, Y.; Nguyen, T.-Q.; Aramaki, S.; Bazan, G. C. *J. Am. Chem. Soc.* **2014**, *136*, 12576.

(7) (a) Bronstein, H.; Chen, Z.; Ashraf, R. S.; Zhang, W.; Du, J.; Durrant, J. R.; Shakya Tuladhar, P.; Song, K.; Watkins, S. E.; Geerts, Y.; Wienk, M. M.; Janssen, R. A. J.; Anthopoulos, T.; Sirringhaus, H.; Heeney, M.; McCulloch, I. *J. Am. Chem. Soc.* **2011**, *133*, 3272. (b) Dou, L.; Chang, W.-H.; Gao, J.; Chen, C.-C.; You, J.; Yang, Y. *Adv. Mater.* **2013**, *25*, 825. (c) Hendriks, K. H.; Li, W.; Wienk, M. M.; Janssen, R. A. J. *J. Am. Chem. Soc.* **2014**, *136*, 12130.

(8) (a) Liu, Y.; Wan, X.; Wang, F.; Zhou, J.; Long, G.; Tian, J.; Chen, Y. *Adv. Mater.* **2011**, *23*, 5387. (b) Zhou, J.; Zuo, Y.; Wan, X.; Long, G.; Qian, Z.; Ni, W.; Liu, Y.; Li, Z.; He, G.; Li, C.; Kan, B.; Li, M.; Chen, Y. *J. Am. Chem. Soc.* **2013**, *135*, 8484. (c) Zhang, Q.; Bin, K.; Liu, F.; Long, G.; Wan, X.; Chen, X.; Zuo, Y.; Ni, W.; Zhang, H.; Li, M.; Hu, Z.; Huang, F.; Cao, Y.; Liang, Z.; Zhang, M.; Russell, T. P.; Chen, Y. *Nat. Photonics* **2014**, 1. (d) Liu, Y.; Chen, C.-C.; Hong, Z.; Gao, J.; Michael Yang, Y.; Zhou, H.; Dou, L.; Li, G.; Yang, Y. *Sci. Rep.* **2013**, *3*, 3356.

(9) (a) Coughlin, J. E.; Henson, Z. B.; Welch, G. C.; Bazan, G. C. *Acc. Chem. Res.* **2014**, *47*, 257. (b) Lin, Y.; Ma, L.; Li, Y.; Liu, Y.; Zhu, D.; Zhan, X. *Adv. Energy Mater.* **2013**, *3*, 1166. (c) Walker, B.; Tamayo, A. B.; Dang, X.-D.; Zalar, P.; Seo, J. H.; Garcia, A.; Tantiwiwat, M.; Nguyen, T.-Q. *Adv. Funct. Mater.* **2009**, *19*, 3063. (d) Wang, H.; Liu, F.; Bu, L.; Gao, J.; Wang, C.; Wei, W.; Russell, T. P. *Adv. Mater.* **2013**, *25*, 6519. (e) van der Poll, T. S.; Love, J. A.; Nguyen, T.-Q.; Bazan, G. C. *Adv. Mater.* **2012**, *24*, 3646. (f) Lee, O. P.; Yiu, A. T.; Beaujuge, P. M.; Woo, C. H.; Holcombe, T. W.; Millstone, J. E.; Douglas, J. D.; Chen, M. S.; Fréchet, J. M. J. *Adv. Mater.* **2011**, *23*, 5359. (g) Qin, H.; Li, L.; Guo, F.; Su, S.; Peng, J.; Cao, Y.; Peng, X. *Energy Environ. Sci.* **2014**, *7*, 1397. (h) Takacs, C. J.; Sun, Y.; Welch, G. C.; Perez, L. A.; Liu, X.; Wen, W.; Bazan, G. C.; Heeger, A. J. *J. Am. Chem. Soc.* **2012**, *134*, 16597. (i) Loser, S.; Bruns, C. J.; Miyauchi, H.; Ortiz, R. P.; Facchetti, A.; Stupp, S. I.; Marks, T. J. *J. Am. Chem. Soc.* **2011**, *133*, 8142. (j) Li, L.; Huang, Y.; Peng, J.; Cao, Y.; Peng, X. *J. Mater. Chem. A* **2013**, *1*, 2144. (k) Sun, Y.; Welch, G. C.; Leong, W. L.; Takacs, C. J.; Bazan, G. C.; Heeger, A. J. *Nat. Mater.* **2011**, *11*, 44.

(10) Kadish, K. M.; Smith, K. M.; Guilard, R. *The Porphyrin Handbook*; Academic Press: San Diego, CA, 1999.

(11) (a) Braunecker, W. A.; Oosterhout, S. D.; Owczarczyk, Z. R.; Larsen, R. E.; Larson, B. W.; Ginley, D. S.; Boltalina, O. V.; Strauss, S. H.; Kopidakis, N.; Olson, D. C. *Macromolecules* **2013**, *46*, 3367. (b) Huang, Y.; Li, L.; Peng, X.; Peng, J.; Cao, Y. *J. Mater. Chem.* **2012**, *22*, 21841.

(12) (a) Spano, F. C. *Acc. Chem. Res.* **2010**, *43*, 429. (b) Shin, W.; Yasuda, T.; Watanabe, G.; Yang, Y. S.; Adachi, C. *Chem. Mater.* **2013**, *25*, 2549. (c) Dautel, O. J.; Wantz, G.; Almairac, R.; Flot, D.; Hirsch, L.; Lere-Porte, J.-P.; Parneix, J.-P.; Serein-Spirau, F.; Vignau, L.; Moreau, J. J. E. *J. Am. Chem. Soc.* **2006**, *128*, 4892.

(13) Shen, S.; Jiang, P.; He, C.; Zhang, J.; Shen, P.; Zhang, Y.; Yi, Y.; Zhang, Z.; Li, Z.; Li, Y. *Chem. Mater.* **2013**, *25*, 2274.

(14) Hiramoto, M.; Kitada, K.; Iketaki, K.; Kaji, T. *Appl. Phys. Lett.* **2011**, *98*, 023302.

(15) Mihailetchi, V. D.; Xie, H. X.; de Boer, B.; Koster, L. J. A.; Blom, P. W. M. *Adv. Funct. Mater.* **2006**, *16*, 699.

(16) (a) Janssen, R. A. J.; Nelson, J. *Adv. Mater.* **2012**, *25*, 1847. (b) Lu, Y.; Xiao, Z.; Yuan, Y.; Wu, H.; An, Z.; Hou, Y.; Gao, C.; Huang, J. *J. Mater. Chem. C* **2013**, *1*, 630.

DOI: 10.1021/jacs.5b03740
J. Am. Chem. Soc. 2015, 137, 7282−7285